JOURNAL OF GUIDANCE, CONTROL, AND DYNAMICS
Vol. 22, No. 6, November–December 1999

Aircraft Handling Qualities and Pilot-Induced Oscillation Tendencies with Actuator Saturation

Yasser Zeyada,* Ronald A. Hess,† and Wichai Siwakosit‡
University of California, Davis, California 95616

A pilot/vehicle analysis technique is offered that can provide predictions of handling-qualities levels and pilot-induced oscillation rating levels in single-axis tracking tasks, with linear or nonlinear vehicle dynamics. The technique is applied to the three vehicle configurations evaluated in the series of flight tests sponsored by the U.S. Air Force that are identified as HAVE LIMITS. The ability of the analysis technique to provide excellent quantitative predictions of the effects of actuator rate saturation on the handling qualities and pilot-induced oscillation susceptibility of the aircraft configurations is demonstrated. An interactive computer code is discussed that automates much of the pilot/vehicle analysis.

Introduction

ONE important problem in the design of flight-control systems for aircraft under piloted control is the determination of handling qualities and pilot-induced oscillation (PIO) tendencies when significant nonlinearities exist in the vehicle description. The most common and troublesome of these nonlinearities is actuator saturation, particularly rate saturation.[1] Until recently, there existed no unifying theory to relate the linear and nonlinear handling qualities and PIO phenomena, although a number of useful analytical tools have been available to tackle the linear problems.[2–5] This analytical shortfall can be attributed to two causes: first, the lack of a pilot model of sufficient validity and flexibility to permit a closed-loop perspective to be used in the problem, and second, the lack of an experimental database of sufficient breadth to verify any analytical approaches that might be proposed. The research described here summarizes an effort aimed at providing such a unifying theory. In particular, a recently developed nonlinear pilot modeling approach[6–8] is applied to the analysis of data from a series of U.S. Air Force sponsored flight tests referred to as HAVE LIMITS.[9]

Flight-Test Data

Figure 1 is a block-diagram representation of a pilot model referred to as the structural model of the human pilot. This model and its potential for predicting handling-qualities(HQ) levels and pilot-induced oscillation rating (PIOR) levels for vehicles described by linear dynamics are discussed by Hess.[6] An extension of the linear technique to the study of vehicles described by nonlinear dynamics is discussed by Hess and Stout.[7–8] Unfortunately, at the time their papers were written,[7–8] no experimental database was available with which to verify the theory presented regarding nonlinear PIOs. Since the publication of that paper, the results of the Air Force HAVE LIMITS study have become available.[9] Indeed, some of these data were employed in the Hess and Stout paper,[8] which demonstrates how HQ levels could be predicted for vehicles possessing nonlinear dynamics, particularly actuator rate saturation.

The HAVE LIMITS study utilized the Air Force/CALSPAN NT-33 variable stability aircraft in a series of longitudinal tracking tasks that used a head-up display with a pair of pitch-and-roll-command tracking tasks. As in the HAVE LIMITS study, it is the pitch-command task that will be of interest here. Two inputs were utilized in HAVE LIMITS—a sum of sines and a discrete command. The results for the latter input, which was deemed a more realistic task by the evaluation pilots,[9] is used herein.

Three vehicle configurations were used in the HAVE LIMITS study, referred to as 2P, 2D, and 2DU. The latter is of particular interest because it involved a simulated aircraft that possessed an aperiodically divergent mode with a time-to-double amplitude of approximately 0.5 s without stability augmentation. The tracking tasks were conducted with an elevator actuator with simulated rate limits ranging from 157 to 10 deg/s. It should be noted that the 157-deg/s rate limit was not violated in flight tests and hence did not create a nonlinear system.

Analytical Approach

Pilot Model Development

The pilot/vehicle analysis technique discussed here is an extension of that proposed earlier by Hess.[6] No detailed discussion of the structural model will be attempted herein. The reader is referred to Hess's paper[6] for a complete presentation of the model's genesis and its potential as a tool for HQ evaluations. A brief overview of the model-based metrics that constitute the structural model's predictive capabilities in terms of handling qualities and PIO susceptibility will, however, be presented.

Linear Analyses

Referring to Fig. 1, we see that the metric responsible for HQ prediction is the magnitude of the transfer function U_M/C, where U_M is a proprioceptively derived feedback signal in the innermost feedback loop of the pilot model, and C is the command input to the pilot/vehicle system. When normalized by the error gain K_e in the feedforward loop of the model of Fig. 1, a handling-qualities sensitivity function (HQSF) can be defined as

$$\text{HQSF} = |(U_M/C)(j\omega)|(1/K_e) \tag{1}$$

The metric responsible for predicting PIO susceptibility is the normalized power spectral density (PSD) of the same proprioceptively derived signal U_M. Normalization refers to dividing the PSD of U_M $[\Phi_{u_m u_m}(\omega)]$ by K_e^2. In the creation of the pilot model, a crossover frequency of 2.0 rad/s is demanded. There is one possible exception to this rule, and it is discussed in a later section.

Hess[6] demonstrates the utility of the two metrics just described in predicting HQ levels and PIOR levels for a series of flight tests conducted on the NT-33A and Total In-Flight Simulator aircraft. Figure 2 defines the aircraft HQ levels (as used here) on the Cooper–Harper rating scale, and Fig. 3 defines the PIOR levels. It should be noted that the PIOR levels are not in standard use but were created in Hess's paper[6] for the purpose of delineating PIOR rating levels similar to those used in the Cooper–Harper rating scale of Fig. 2. In addition, the definition of level 3 handling qualities in Fig. 2

Received 5 August 1998; presented as Paper 98-4334 at the AIAA Atmospheric Flight Mechanics Conference, Boston, MA, 10–12 August 1998; accepted for publication 8 May 1999.

*Postgraduate Researcher, Department of Mechanical and Aeronautical Engineering.
†Professor, Department of Mechanical and Aeronautical Engineering. Associate Fellow AIAA.
‡Graduate Student, Department of Mechanical and Aeronautical Engineering.

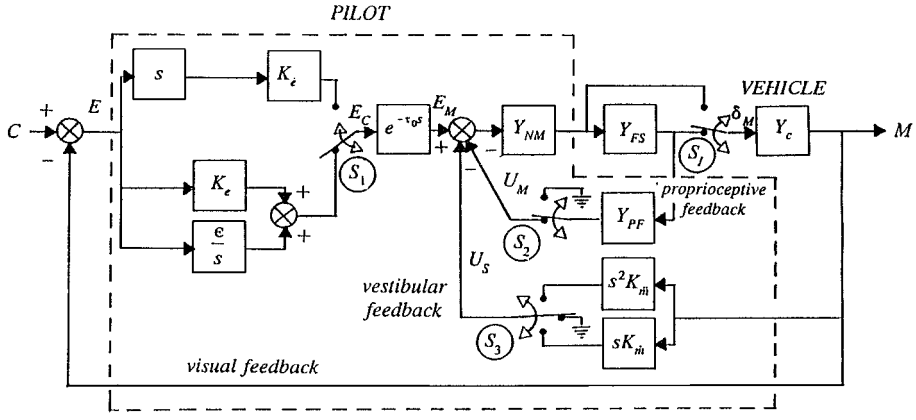

Fig. 1 Structural model of the human pilot.

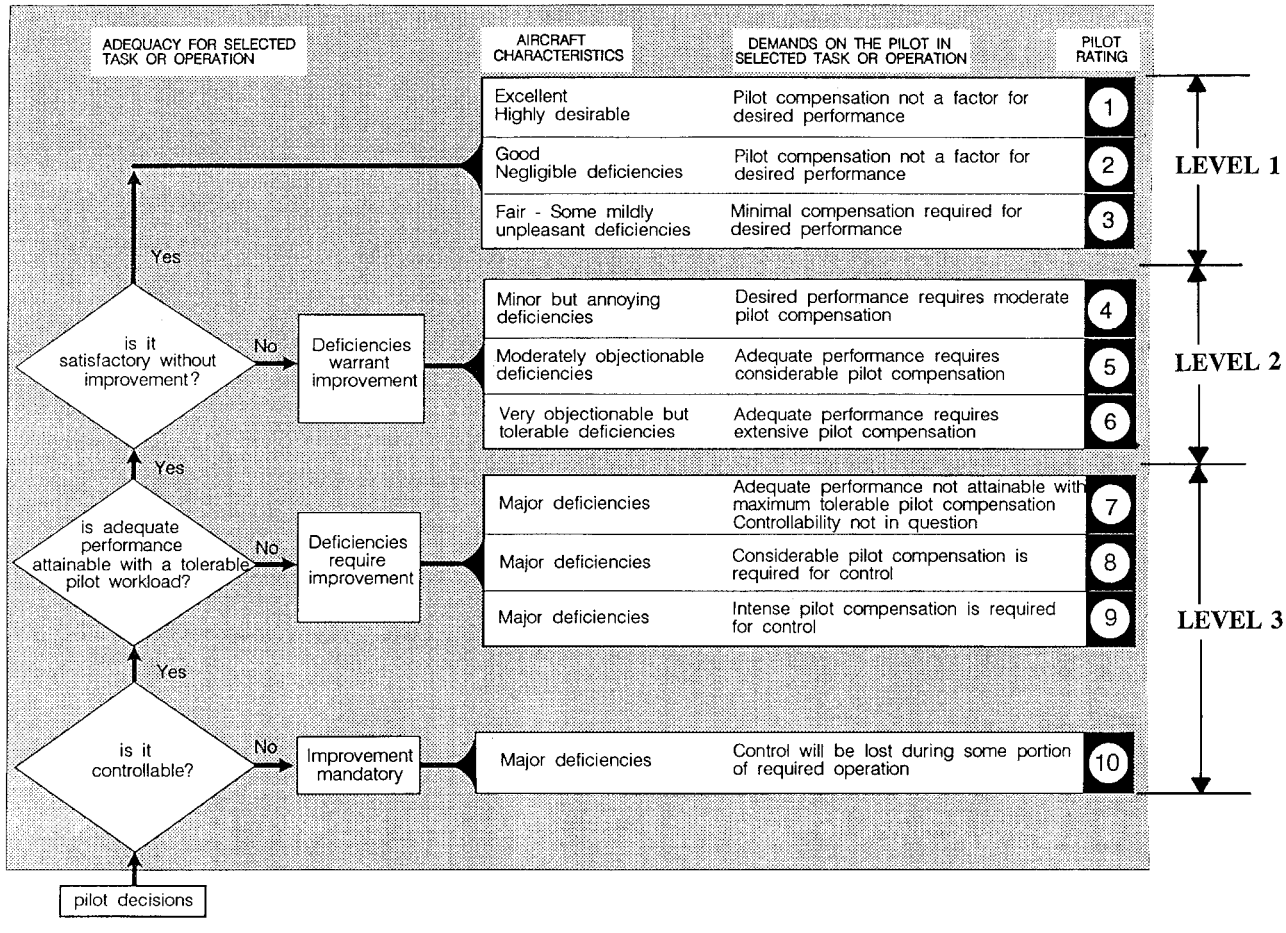

Fig. 2 Cooper–Harper pilot rating scale.

as extending from the Cooper–Harper scale of 6.5 to 10 should be noted. Typically, the definition of level 3 extends only to 8.5, but it was extended to 10 here for convenience. Finally, it should be noted that the scale of Fig. 3 was modified somewhat for the HAVE LIMITS study; that is, a decision-tree approach similar to that employed in the Cooper–Harper scale was used. The scale of Fig. 3 is retained here, because it was this scale that was used in the databases used to develop the PIOR bounds in a figure shown later.

Hess[6] showed that boundaries could be established on plots of the HQSF vs frequency and normalized $\Phi_{u_m u_m}(\omega)$ vs frequency that could successfully delineate HQ levels and PIOR levels. Figures 4 and 5 show these bounds, along with a sample HQSF and normalized $\Phi_{u_m u_m}(\omega)$. The figures are interpreted as follows. Because the HQSF in Fig. 4 enters the area of the figure associated with level 3 handling qualities, the pilot/vehicle system that generated this function is predicted to exhibit level 3 handling qualities. Likewise, because the normalized $\Phi_{u_m u_m}(\omega)$ in Fig. 5 enters the area associated with PIOR ≥ 4, the pilot/vehicle system that generated this function is predicted to exhibit PIORs greater than 4 and to be PIO prone.

A frequency range in which the PIO can be assumed to occur can also be established. First, the lowest frequency at which a peak enters the area associated with PIOR ≥ 4 serves as a lower-frequency boundary. Second, an upper-frequency boundary is established by considering a fundamental change in the pilot's tracking behavior. As discussed in detail by Hess,[6] it is hypothesized that "regressive" tracking behavior occurs in a fully developed PIO in which *error rate* rather than *error* serves as the visual input to the pilot and in which the proprioceptive loop in the model of Fig. 1 is not employed. In terms of Fig. 1, this means that switches S_1 and S_2 move to the "up" position. (No vestibular feedback was assumed in creating the bounds of Figs. 4 and 5; thus switch S_3 remains in the center

DESCRIPTION	NUMERICAL RATING	
NO TENDENCY FOR PILOT TO INDUCE UNDESIRABLE MOTIONS	1	$1 \le PIOR \le 2$
UNDESIRABLE MOTIONS TEND TO OCCUR WHEN PILOT INITIATES ABRUPT MANEUVERS OR ATTEMPTS TIGHT CONTROL. THESE MOTIONS CAN BE PREVENTED OR ELIMINATED BY PILOT TECHNIQUE	2	
UNDESIRABLE MOTIONS EASILY INDUCED WHEN PILOT INITIATES ABRUPT MANEUVERS OR ATTEMPTS TIGHT CONTROL. THESE MOTIONS CAN BE PREVENTED OR ELIMINATED BUT ONLY AT SACRIFICE TO TASK PERFORMANCE OR THROUGH CONSIDERABLE PILOT ATTENTION AND EFFORT	3	$2 < PIOR < 4$
OSCILLATIONS TEND TO DEVELOP WHEN PILOT INITIATES ABRUPT MANEUVERS OR ATTEMPTS TIGHT CONTROL. PILOT MUST REDUCE GAIN OR ABANDON TASK TO RECOVER	4	
DIVERGENT OSCILLATIONS TEND TO DEVELOP WHEN PILOT INITIATES ABRUPT MANEUVERS OR ATTEMPTS TIGHT CONTROL. PILOT MUST OPEN LOOP BY RELEASING OR FREEZING THE STICK	5	$PIOR \ge 4$
DISTURBANCE OR NORMAL PILOT CONTROL MAY CAUSE DIVERGENT OSCILLATION. PILOT MUST OPEN CONTROL LOOP BY RELEASING OR FREEZING THE STICK	6	

Fig. 3 PIOR scale.

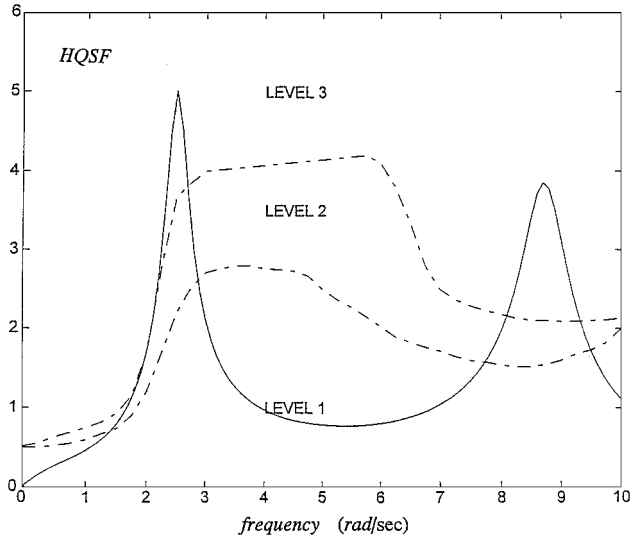

Fig. 4 Example of HQSF showing predicted level 3 handling qualities.

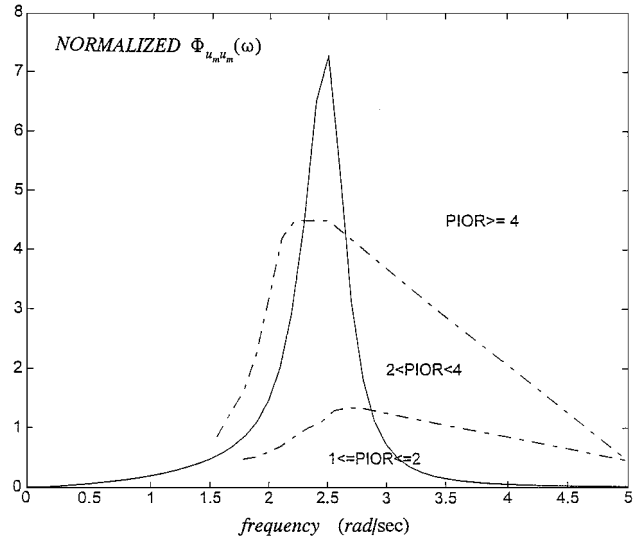

Fig. 5 Example of normalized $\Phi_{u_m u_m}(\omega)$ showing the predicted PIOR $\ge$ 4.

position). Then gain K_e is increased until neutral stability occurs. The frequency of the oscillation establishes the upper boundary for the PIO frequency. The possibility of a range of PIO frequencies is a recognition of the fact that some reported PIOs may not be fully developed, that is, requiring the pilot to release or freeze the inceptor to stop the oscillation.

Nonlinear Simulations

The analysis technique just discussed was limited to vehicles described by linear dynamics. It can, in principle, be extended to systems described by nonlinear dynamics. For linear systems, the HQSF can be uniquely obtained as a transfer function by use of simple block-diagram algebra. For nonlinear systems, however, this is no longer possible, because nonlinear elements (i.e., the "effective vehicle" model) are now in evidence. However, a measurement equivalent to the HQSF can be obtained from a simulation of the nonlinear pilot/vehicle system as follows:

$$\text{HQSF} = \sqrt{\left[\frac{\Phi_{u_m u_m}(\omega)}{\Phi_{cc}(\omega)}\right]}\left|\frac{1}{K_e}\right| \qquad (2)$$

where $\Phi_{u_m u_m}(\omega)$ and $\Phi_{cc}(\omega)$ represent, respectively, the PSDs of $u_m(t)$ and $c(t)$. The HQSF of Eq. (2) can be described as an approximation to the magnitude of the linear transfer function that would produce $u_m(t)$, given $c(t)$ in the nonlinear system. Note that any phase information in this "equivalent" linear transfer function is lost, because only PSDs, as opposed to cross-power spectral densities, are involved. This is no handicap here, however, as the HQSF is defined as a transfer magnitude [see Eq. (1)].

Computationally, Eq. (2) is handled as follows:

$$\text{HQSF} = \frac{\left|\int_0^T u_m(t)e^{-j(\omega t)}\,dt\right|_{\omega=\omega_i}}{\left|\int_0^T c(t)e^{-j(\omega t)}\,dt\right|_{\omega=\omega_i}}\left|\frac{1}{K_e}\right| \qquad i = 1, 2, \ldots, 50 \quad (3)$$

that is, a ratio of Fourier transforms. The upper limit T is chosen to be larger than the duration of the input to the pilot $c(t)$, and such that, for each ω_i, the factor $T/(2\pi/\omega_i)$ is an integer. There are obviously other approaches to obtaining this equivalent HQSF.

As described in the preceding paragraphs, bounds on the HQSF and the normalized $\Phi_{u_m u_m}(\omega)$ that define HQ levels and PIOR levels have been established for linear systems. The question now arises as to their utility for nonlinear systems. The approach taken here is to interpret these bounds for nonlinear systems exactly as for linear systems. That is, let us graphically determine which areas in Figs. 4 and 5 are entered by the curves defined by HQSF vs frequency and normalized $\Phi_{u_m u_m}(\omega)$ vs frequency. In the case of a linear analysis, however, the bounds defining PIOR levels were obtained from the structural model by using a specific input, that is, a random input with a PSD given by[6]

$$\Phi_{cc}(\omega) = \frac{4^2}{\omega^4 + 4^2} \tag{4}$$

Because Eq. (4) was to be used in a linear analysis, the root mean square (rms) value of $c(t)$ was of no concern, as long as it was invariant. With nonlinear systems, however, the rms value is very important because it can determine the extent to which system nonlinearities are encountered. As a way to accommodate this fact, the normalized $\Phi_{u_m u_m}(\omega)$ for nonlinear analysis was defined as

$$\Phi_{u_m u_m}(\omega)|_{\text{normalized}} = \left[\frac{4^2}{\omega^4 + 4^2}\right] \text{HQSF}^2 \tag{5}$$

with the HQSF obtained from Eq. (3). The inclusion of the bracketed PSD in Eq. (5) with the HQSF from a simulation of the nonlinear pilot/vehicle system allows the linear PIOR bounds to be used in a nonlinear analysis with any input $c(t)$.

Computational Aid

Zeyada and Hess[10] describe a computer-aided analysis tool that was used in the analytical investigation to be described. The tool is referred to as Pilot/Vehicle Dynamics$_{\text{NonLinear}}$ (PVD$_{\text{NL}}$) and is based upon MATLAB, the Control System Toolbox, and Simulink. This program automates much of the structural model analysis procedure that was described herein.

HAVE LIMITS Configurations and Flight-Test Results

Figure 6 is a block-diagram representation of the flight-control systems utilized in the HAVE LIMITS study. Table 1 provides more detailed information about the vehicle dynamics. By appropriate selection of the feedback gains K_{α_1}, K_{q_1}, K_{α_2}, and K_{q_2}, the three vehicle configurations defined as 2P, 2D, and 2DU were created. The feedback gains for 2P and 2D are seen in Table 1 to be identical. The two configurations differ in that a first-order filter was added to the forward path of 2P just after the force/feel system. In addition, as noted by Mitchell et al.,[11] there existed additional configuration-dependent delays in the flight-control system. These delays are noted in the block diagram of Fig. 6 and in Table 1. Figure 7 shows the discrete pitch-attitude command used. Table 2 summarizes the HQ ratings (HQRs) and PIORs achieved with one of the three evaluation pilots, across the three vehicle configurations employing the elevator actuator rate limits indicated. This particular pilot's data were selected for comparison here because Mitchell et al.[11] identified this pilot as the one who "flew aggressively and seemed most sensitive to small changes in aircraft dynamics and rate limiting."

Analytical/Simulation Results

Table 1 shows the bare-airframe dynamics of the NT-33A, as well as the feedback gains in the variable-stability setup of Fig. 6 that produced the three flight test configurations. Also shown are the effective transfer functions, $(\theta/\delta_{e_c})(s)$ in Fig. 6, for these configurations.

In addition to the elevator rate limiting, the pilot/vehicle simulations with the structural model also included elevator amplitude limits of ± 20 deg. In the figures that follow, legends and curves identified as "analysis" are the pilot/vehicle modeling results when no nonlinearities (elevator rate and amplitude limiting) were included in the vehicle model, and when linear transfer functions and PSD relations were used to obtain the curves shown. Those identified as "simulation" included these nonlinearities, and the results were obtained by utilizing time histories obtained from Simulink simulations, using Eqs. (3) and (5). This allows a quick evaluation of the

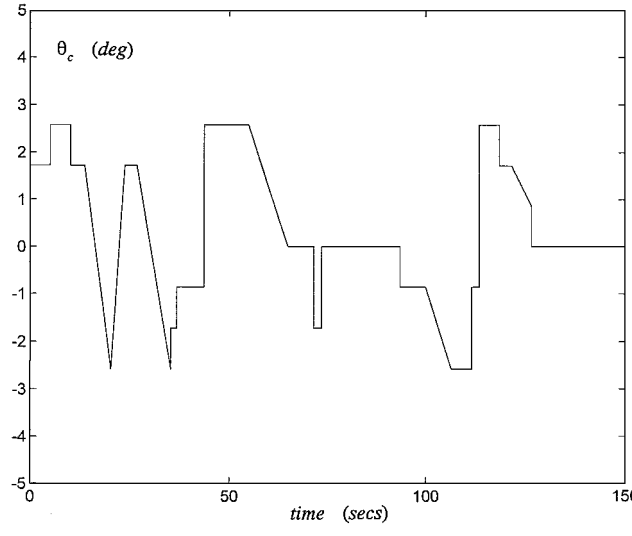

Fig. 7 Discrete pitch-attitude input for the HAVE LIMITS flight test.

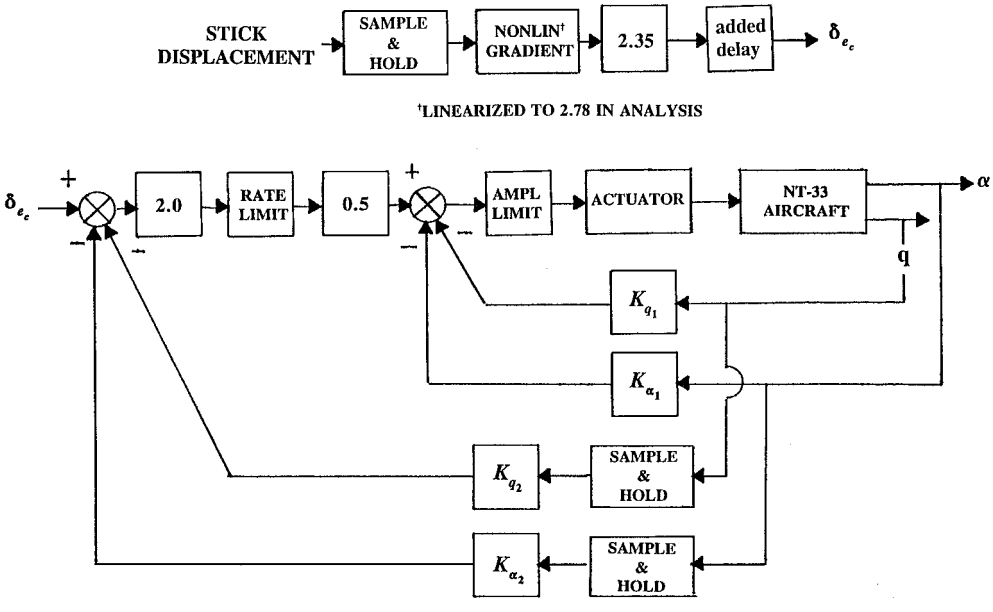

Fig. 6 Flight-control system for the HAVE LIMITS flight test.

Table 1 HAVE LIMITS configuration definitions

Parameter	Description
NT-33A dynamics (no feedbacks)	$\dot{x}(t) = Ax(t) + Bu(t)$
	$x = [u(\text{ft/s}), \alpha(\text{deg}), q(\text{deg/s}), \theta(\text{deg})]^T$
	$u = \delta_e(\text{deg})$ positive trailing edge up
	$A = \begin{bmatrix} -0.033104 & 0.14957 & -0.3207 & -0.56111 \\ -0.015511 & -1.2826 & 1.0 & -0.0024621 \\ 0.008081 & -4.0875 & -1.7556 & 0.0012828 \\ 0 & 0 & 1.0 & 0 \end{bmatrix}$
	$B = [0.5193 \quad 0.05243 \quad 11.085 \quad 0]^T$
Feedback gains	
Configuration 2P[a]	
K_{α_1}	1
K_{α_2}	0
K_{q_1}	0.32
K_{q_2}	0
Configuration 2D	
K_{α_1}	1
K_{α_2}	0
K_{q_1}	0.32
K_{q_2}	0
Configuration 2DU	
K_{α_1}	−0.6
K_{α_2}	1.6
K_{q_1}	−0.2
K_{q_2}	0.52
Actuator	$\frac{75^2}{s^2 + 2(0.7)(75)s + 75^2}$
Force/feel system	$\frac{24.07}{s^2 + 2(0.65)(23)s + 23^2}$ in./lbf
Approximate pitch-attitude dynamics $[(\theta/\delta_{e_c})$ deg/deg]	
Configuration 2P	$\frac{260(s+1.3)e^{-0.064s}}{s(s+4)[s^2 + 2(0.71)(4.82)s + 4.82^2]}$
Configuration 2D	$\frac{59.6(s+1.3)e^{-0.058s}}{s[s^2 + 2(0.66)(4.64)s + 4.64^2]}$
Configuration 2DU	$\frac{69.8(s+1.3)e^{-0.07s}}{s[s^2 + 2(0.56)(4.75)s + 4.75^2]}$

[a]A first-order filter $4/(s+4)$ was added just after the force/feel system to create 2P from 2D.

Table 2 Cooper–Harper and PIORs for a single pilot in the HAVE LIMITS flight test—discrete task

	Rating for elevator rate limit (deg/s)				
Configuration	157	60	40	20	10
2P					
HQR	4		5/5	7/3	
PIOR	2		3/3	4/1	
2D					
HQR	4		1/2	2	6
PIOR	2		1/2	2	3
2DU					
HQR	5/4	10/10			
PIOR	3/2	5/5			

effects of the nonlinearities on predicted handling qualities and PIO susceptibility.

Configuration 2P

Figure 8 shows the open-loop pilot/vehicle transfer function (M/E in Fig. 1) produced by PVD_{NL}. This figure demonstrates a phenomenon that can occur in pilot/vehicle analyses, namely, the existence of a relatively flat amplitude portion of the Bode diagram of the open-loop pilot/vehicle system. This was caused by the inclusion of an effective lead term in the pilot model [causing $Y_{PF} \propto 1/(s+4)$ in Fig. 1 to cancel the lag introduced in the vehicle dynamics by the filter noted in Table 2]. As discussed by Hess[6] and Zeyada and Hess,[10] pilot/vehicle dynamics such as these pose problems when the 2.0-rad/s crossover frequency alluded to in the preceding paragraphs is enforced. Namely, small changes in pilot gain will result in large decrements in stability margins. Thus, they believed that enforcing the 2.0-rad/s frequency would be unrealistic.

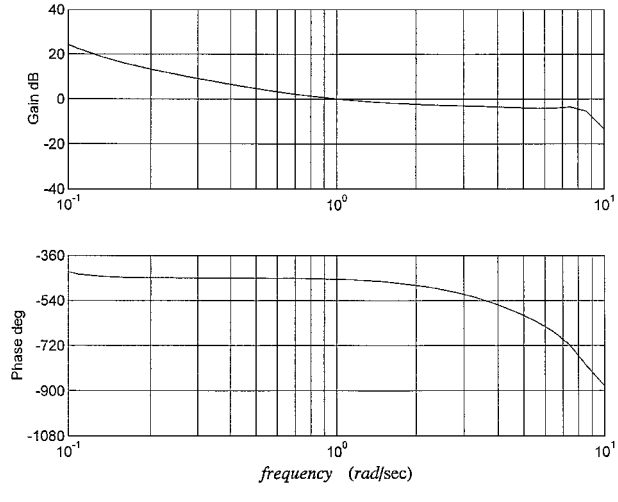

Fig. 8 Structural model pilot/vehicle transfer function (M/E) for configuration 2P.

They did propose an approach to alleviate this problem: Increase the crossover frequency until the offending flat portion of the amplitude plot is at least 2.0 dB above the 0-dB line. If this change cannot be accomplished with positive stability margins, the crossover frequency should be reduced to 1.0 rad/s. The latter change was employed for configuration 2P. Figures 9–14 show the HQSF and normalized $\Phi_{u_m u_m}(\omega)$ plots for elevator rate limits of 157, 40, and 20 deg/s. For convenience, the flight-test HQRs and PIORs from Table 1 are repeated in the figures.

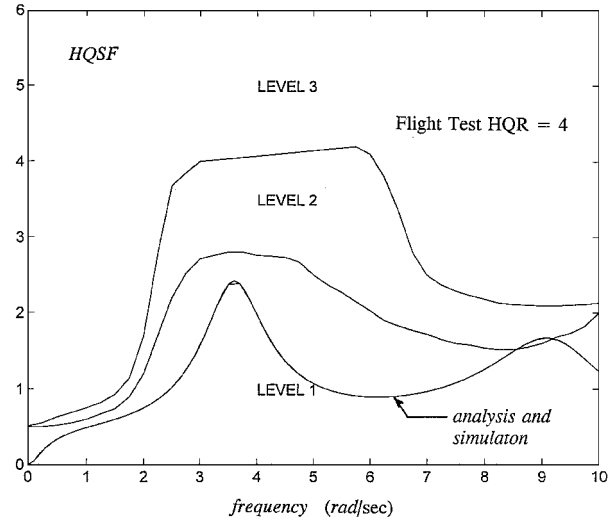

Fig. 9 HQSF for configuration 2P, with a 157-deg/s elevator rate limit.

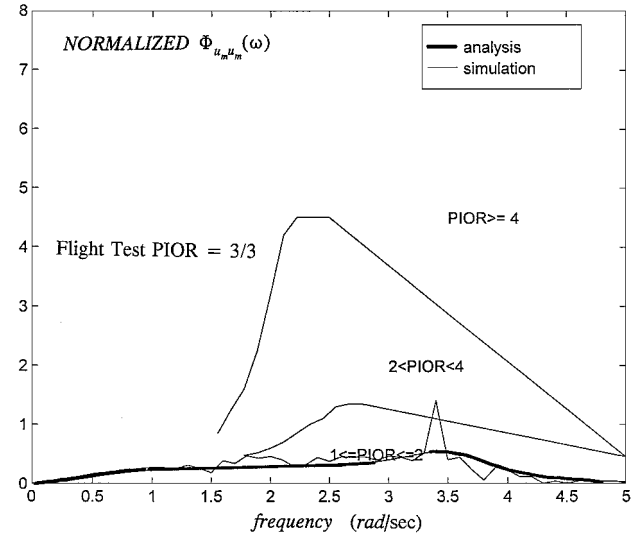

Fig. 12 Normalized $\Phi_{u_m u_m}(\omega)$ for configuration 2P, with a 40-deg/s elevator rate limit.

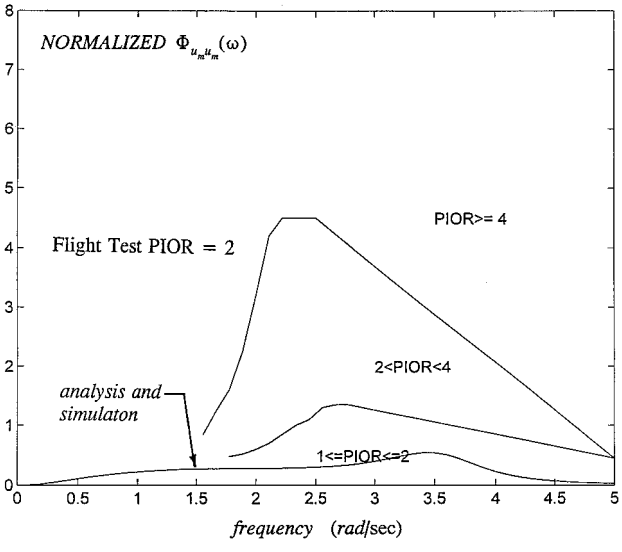

Fig. 10 Normalized $\Phi_{u_m u_m}(\omega)$ for configuration 2P, with a 157-deg/s elevator rate limit.

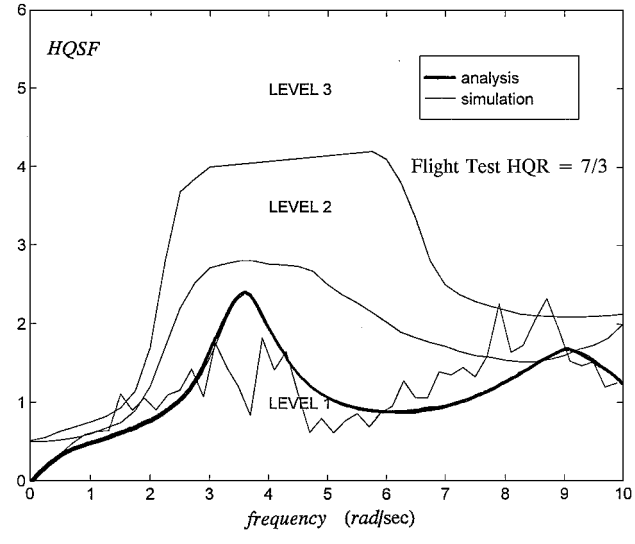

Fig. 13 HQSF for configuration 2P, with a 20-deg/s elevator rate limit.

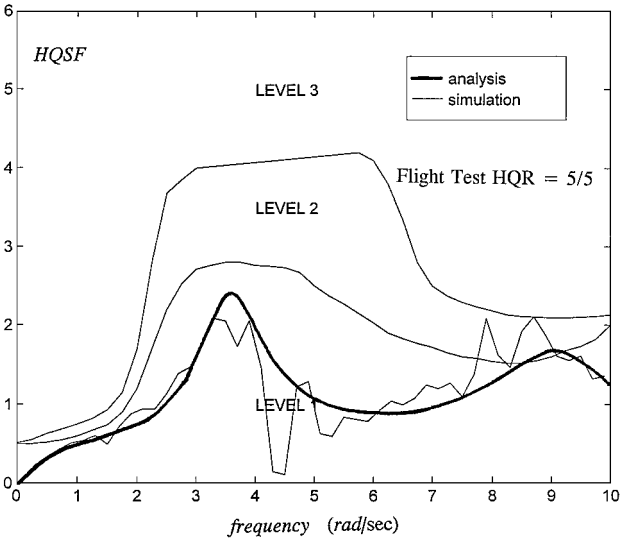

Fig. 11 HQSF for configuration 2P, with a 40-deg/s elevator rate limit.

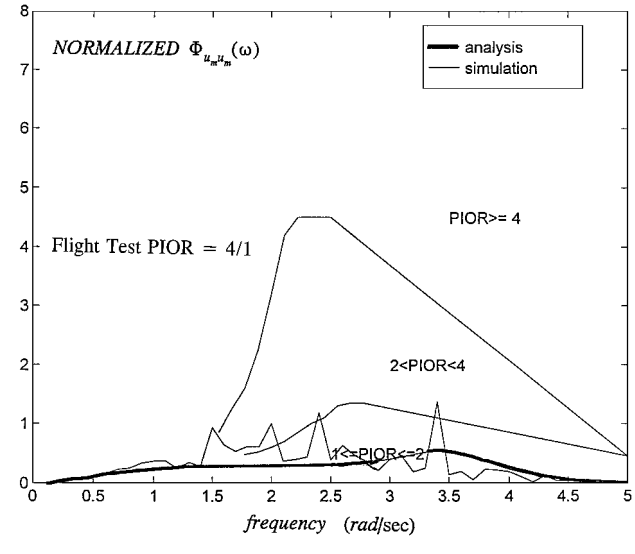

Fig. 14 Normalized $\Phi_{u_m u_m}(\omega)$ for configuration 2P, with a 20-deg/s elevator rate limit.

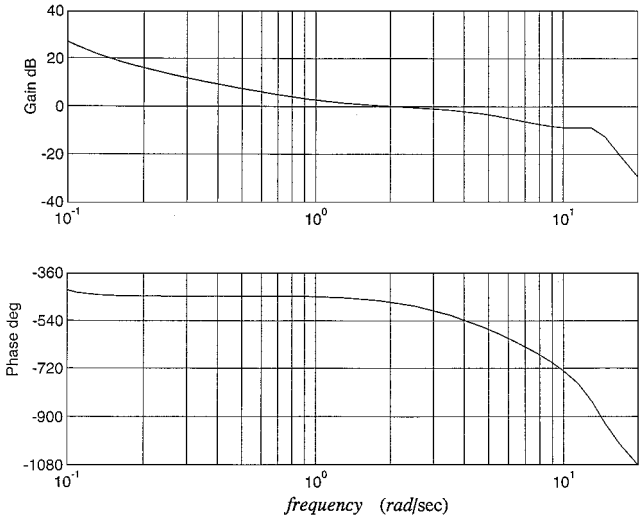

Fig. 15 Structural model pilot/vehicle transfer function (*M/E*) for configuration 2D.

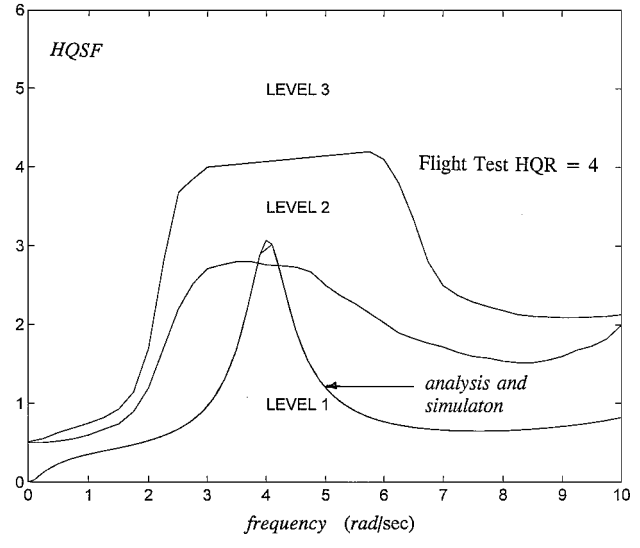

Fig. 16 HQSF for configuration 2D, with a 157-deg/s elevator rate limit.

Configuration 2D

Figure 15 shows the open-loop pilot/vehicle transfer function produced by PVD_{NL}. Figures 16–23 show the HQSF and normalized $\Phi_{u_m u_m}(\omega)$ plots for elevator rate limits of 157, 40, 20, and 10 deg/s. The additional 10-deg/s rate limit was investigated here because, as Table 1 indicates, the flight-test HQ ratings returned to the level 2 ratings obtained with the 157-deg/s rate limits but with a PIOR of 3.

Configuration 2DU

Figure 24 shows the open-loop pilot/vehicle transfer function produced by PVD_{NL}. Figures 25–28 show the HQSF and normalized $\Phi_{u_m u_m}(\omega)$ plots for elevator rate limits of 157 and 60 deg/s. The analytical pilot/vehicle system was unstable for any elevator rate limit less than 53 deg/s.

Discussion

Flight-test pilot ratings are indicated in Table 2 and on the appropriate figures. In cases in which more than one flight-test rating was given by the pilot, the rating indicating the highest numerical rating was used in a comparison with model results. Of the 18 combinations of configurations, rate limits, and characteristics rated (HQR or PIOR), the structural model as implemented in PVD_{NL} correctly predicted the HQ level and PIOR level for 14. The four failures were 1) the predicted PIOR level for configuration 2P with a

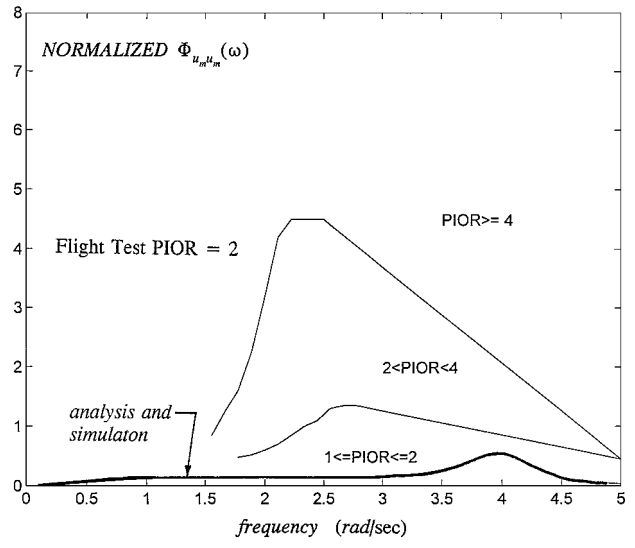

Fig. 17 Normalized $\Phi_{u_m u_m}(\omega)$ for configuration 2D, with a 157-deg/s elevator rate limit.

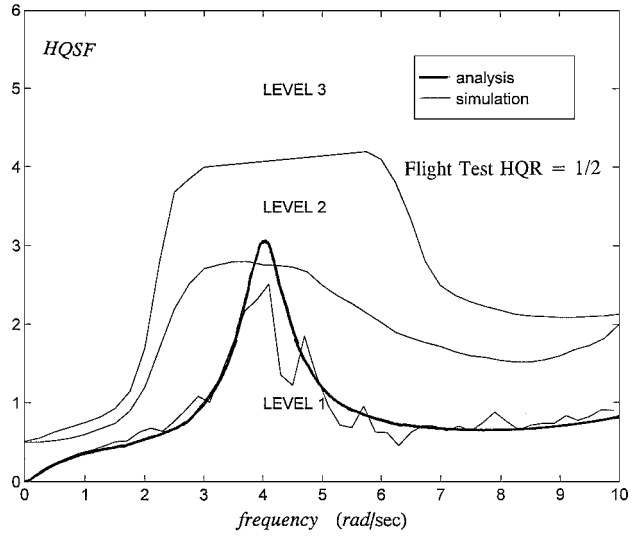

Fig. 18 HQSF for configuration 2D, with a 40-deg/s elevator rate limit.

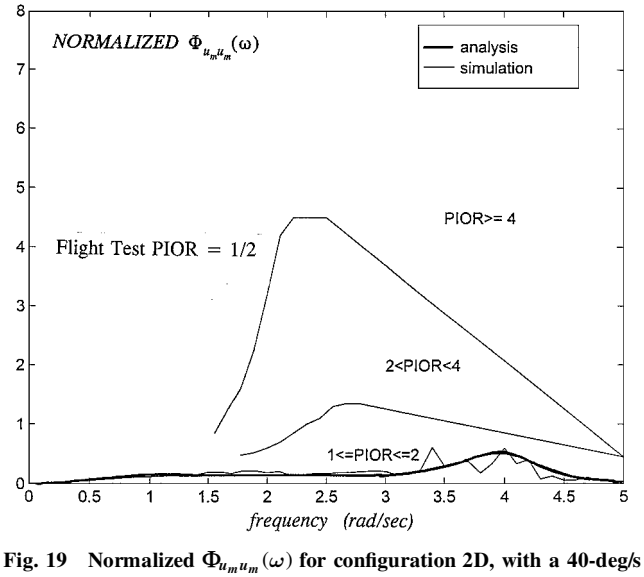

Fig. 19 Normalized $\Phi_{u_m u_m}(\omega)$ for configuration 2D, with a 40-deg/s elevator rate limit.

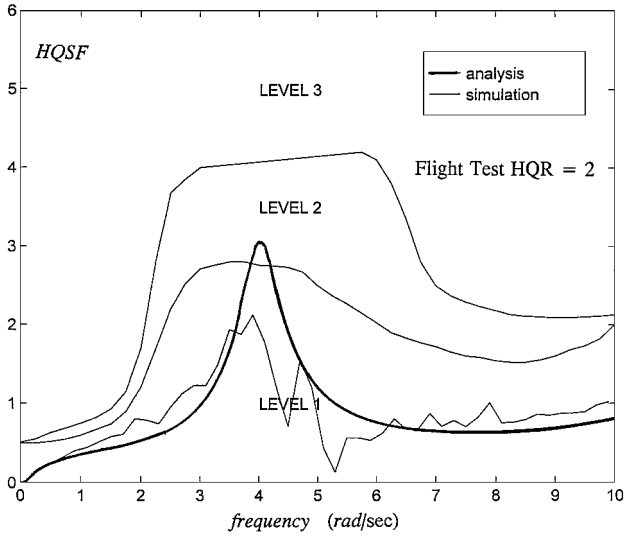

Fig. 20 HQSF for configuration 2D, with a 20-deg/s elevator rate limit.

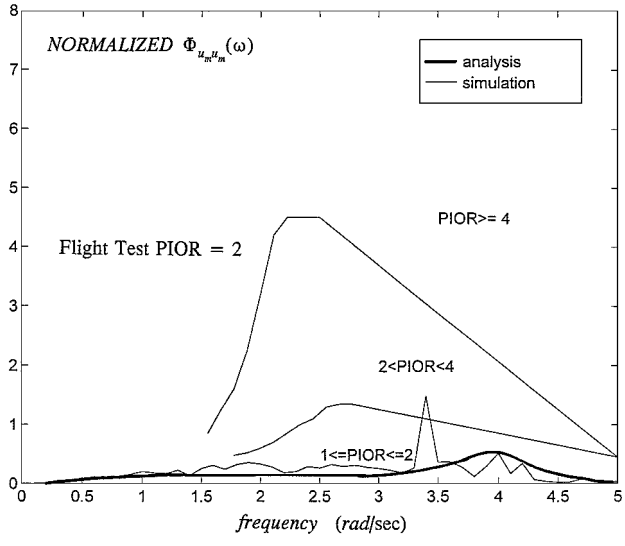

Fig. 21 Normalized $\Phi_{u_m u_m}(\omega)$ for configuration 2D, with a 20-deg/s elevator rate limit.

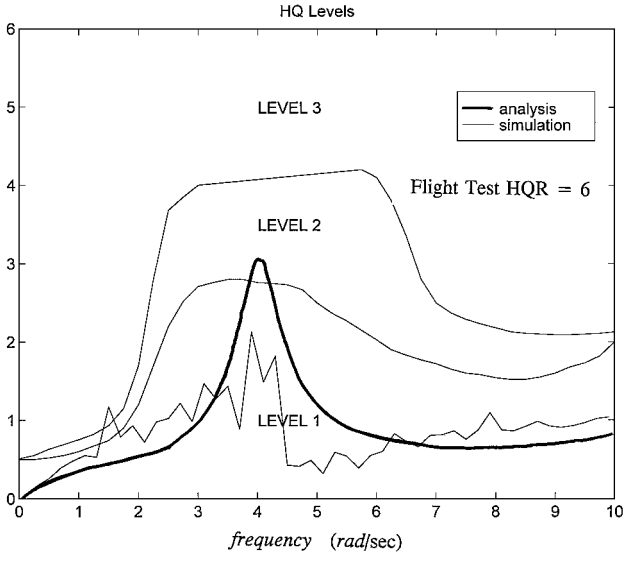

Fig. 22 HQSF for configuration 2D, with a 10-deg/s elevator rate limit.

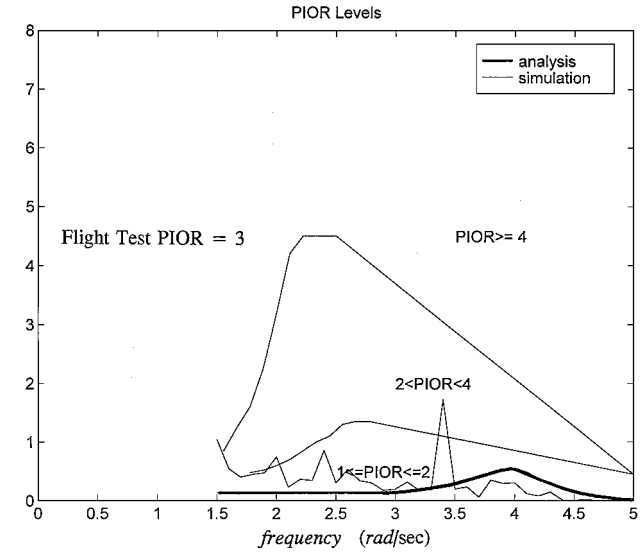

Fig. 23 Normalized $\Phi_{u_m u_m}(\omega)$ for configuration 2D, with a 10-deg/s elevator rate limit.

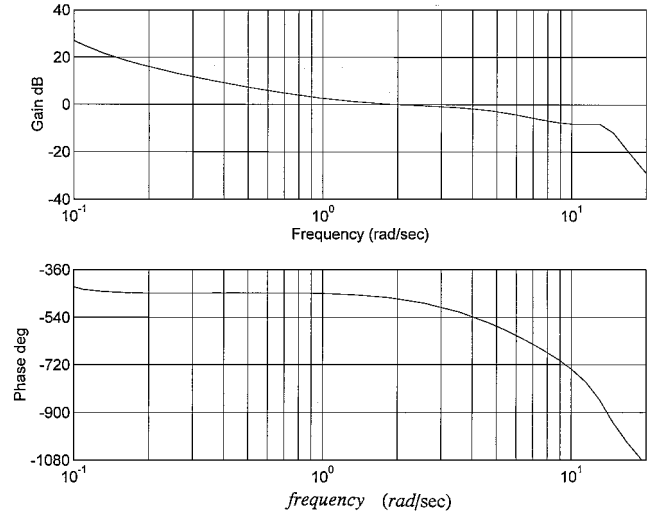

Fig. 24 Structural model pilot/vehicle transfer function (M/E) for configuration 2DU.

20-deg/s rate limit (predicted $2 < \text{PIOR} < 4$; flight-test PIOR = 4); 2) the predicted PIOR level for configuration 2D with a 20-deg/s rate limit (predicted $2 < \text{PIOR} < 4$; flight-test PIOR = 2); 3) configuration 2DU with a 157-deg/s rate limit (predicted $1 \leq \text{PIOR} \leq 2$; flight-test PIOR = 3); and 4) predicted HQ level for configuration 2D with a 10-deg/s rate limit (predicted level 3 handling qualities; flight-test HQR = 6). Finally, the inability of the structural model to control configuration 2DU with rate limits below 53 rad/s is corroborated by the HQRs for which Cooper–Harper ratings of 10 were given for all configurations with rate limits at or below 60 deg/s.

As with any nonlinear system, the choice of input can have a significant effect upon the behavior of the system. Here the choice of input was dictated by that used in the HAVE LIMITS flight test. In a situation in which the analyst is exercising the modeling procedure in which no specific flight test is being emulated, the choice of input can be critical. In this case, a conservative approach would be to use a broadband randomly appearing input (as in Ref. 7) that creates cockpit inceptor motion (force) approaching the limit of control authority.

PIOs

It is of some interest to investigate conditions in which PIOs occurred in flight tests. Configuration 2DU offers ample evidence of a configuration that was highly PIO prone in the presence of rate saturation. Kish's investigation[9] indicates that with 50-deg/s elevator

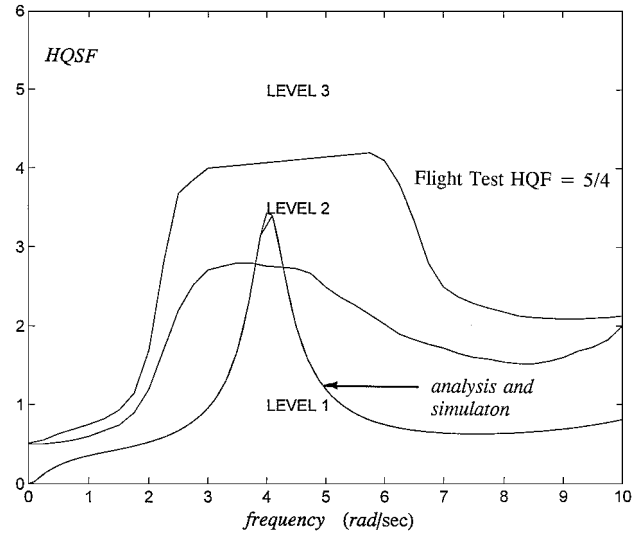

Fig. 25 HQSF for configuration 2DU, with a 157-deg/s elevator rate limit.

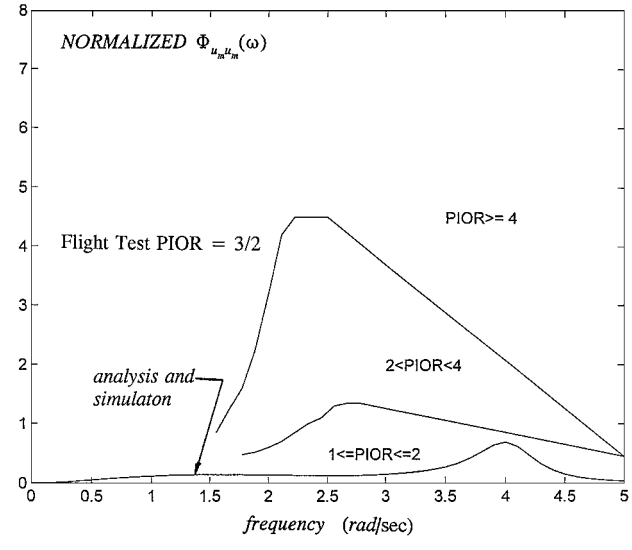

Fig. 26 Normalized $\Phi_{u_m u_m}(\omega)$ for configuration 2DU, with a 157-deg/s elevator rate limit.

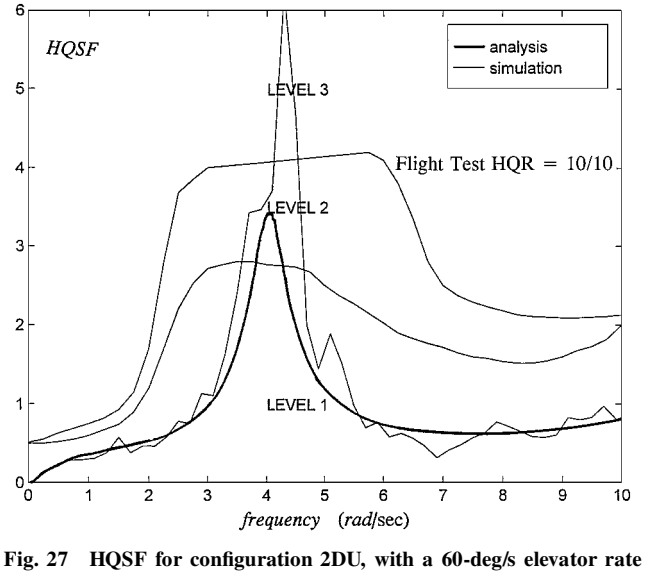

Fig. 27 HQSF for configuration 2DU, with a 60-deg/s elevator rate limit.

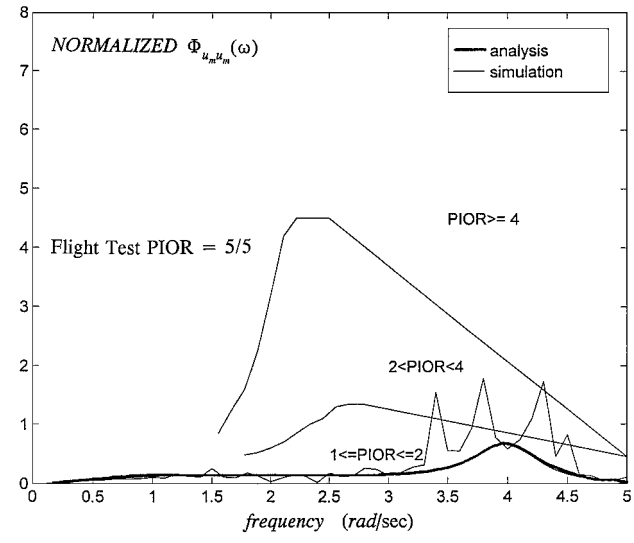

Fig. 28 Normalized $\Phi_{u_m u_m}(\omega)$ for configuration 2DU, with a 60-deg/s elevator rate limit.

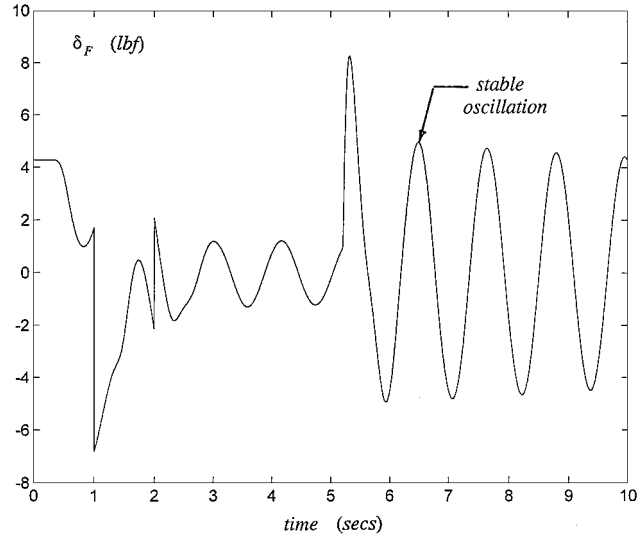

Fig. 29 Structural model "regressive" behavior showing a pilot-induced oscillation.

rate saturation, configuration 2DU received PIORs of 5 from the pilot selected herein for comparison. This PIOR along with the pilot comments reported by Kish suggest that these PIOs may have been in the "fully developed" category. A perusal of tracking records appearing in Kish's report for this pilot and configuration indicated large pitch-attitude overshoots and oscillations appearing at those times when abrupt, large-amplitude pitch commands were encountered (e.g., at approximately 42 and 107 s in the pitch command of Fig. 7). The frequency of these oscillations was approximately 5.3 rad/s.

The pilot was next modeled in the "regressive" tracking mode. The input of Fig. 7 was deleted, and a doublet, force disturbance was injected into δ_F in Fig. 1 to excite the system. The doublet had a duration of 2 s and an amplitude equal to the rms value of the structural model inceptor force measured in the previous nonlinear simulation with the input of Fig. 7. The minimum stable actuator rate limit of 53 deg/s was used. Adjusting the gain $K_{\dot{e}}$ to the point of neutral stability led to the 5.4-rad/s oscillation indicated in Fig. 29. This compares well with the 5.3-rad/s value gleaned from the flight-test record.

Limitations

Two important limitations of the pilot/vehicle analysis procedure discussed here must be emphasized. First, handling qualities and PIO predictions will not reflect changes in control sensitivity. This

is because the metrics responsible for these predictions have been normalized by the pilot gain K_e [Eqs. (1–3)]. Second, nonlinear inceptor gradients must be linearized to allow stable structural model behavior. This is equivalent to assuming that the pilot inverts nonlinear inceptor gradients in tracking.

Conclusions

A unifying theory for handling qualities and pilot-induced oscillation tendencies can be offered for both linear and nonlinear systems. A structural pilot model, implemented in a computer-aided design program, provided predictions of handling qualities levels and pilot-induced oscillation levels that compared quite well with those from flight tests. The model generated predictions agreeing with flight-test results in 14 out of 18 cases analyzed.

References

[1]Aviation Safety and Pilot Control—Understanding and Preventing Unfavorable Pilot-Vehicle Interactions, *Report of the Committee on the Effects of Aircraft-Pilot Coupling on Flight Safety*, National Academy Press, Washington, DC, 1997, pp. 19–29.

[2]Neal, T. P., and Smith, R. E., "An In-Flight Investigation to Develop Control System Design Criteria for Fighter Airplanes," Air Force Flight Dynamics Lab., AFFDL-TR-70-74, Wright–Patterson AFB, OH, Dec. 1970.

[3]Smith, R. H., and Geddes, N. D., "Handling Qeality Requirements for Advanced Aircraft Design: Longitudinal Mode," Air Force Flight Dynamics Lab., AFFDL-TR-78-154, Wright–Patterson AFB, OH, Aug. 1979.

[4]Gibson, J. C., "Piloted Handling Qualities Criteria for High Order Flight Control Systems," *Criteria for Handling Qualities of Military Aircraft*, CP-333, AGARD, April 1982, pp. 4-1–4-15.

[5]Hoh, R. H., Mitchell, D. G., and Hodgkinson, J., "Bandwidth—A Criterion for Highly Augmented Airplanes," *Criteria for Handling Qualities of Military Aircraft*, CP-333, AGARD, April 1982, pp. 9-1–9-11.

[6]Hess, R. A., "A Unified Theory for Aircraft Handling Qualities and Adverse Aircraft-Pilot Coupling," *Journal of Guidance, Control, and Dynamics*, Vol. 20, No. 6, 1997, pp. 1141–1148.

[7]Hess, R. A., and Stout, P. W., "Assessing Aircraft Susceptibility to Nonlinear Aircraft-Pilot Coupling/Pilot Induced Oscillations," *Journal of Guidance, Control, and Dynamics*, Vol. 21, No. 6, 1998, pp. 957–964.

[8]Hess, R. A., and Stout, P. W., "Predicting Handling Qualities Levels for Vehicles with Nonlinear Dynamics," AIAA Paper 98-0494, Jan. 1998.

[9]Kish, B. A., "A Limited Flight Test Investigation of Pilot-Induced Oscillation Due to Elevator Rate Limiting," Air Force Flight Test Center, AFFTC-TR-97-12, Edwards, CA, Aug. 1997.

[10]Zeyada, Y., and Hess, R. A., "PVD$_{NL}$—Pilot/Vehicle Dynamics$_{NonLinear}$; An Interactive Computer Program for Modeling the Human Pilot in Single-Axis Linear and Nonlinear Tracking Tasks," Mechanical and Aeronautical Engineering Dept., Univ. of California, Davis, CA, 1998.

[11]Mitchell, D. G., Kish, B. A., and Seo, J. S., "A Flight Investigation of Pilot-Induced Oscillation Due to Rate Limiting," Inst. of Electrical and Electronics Engineers, Paper 270, March 1998.